RSC Advances

ROYAL SOCIETY OF CHEMISTRY

www.rsc.org/advances

Three novel d^7/d^{10} metal complexes with N-heterocyclic ligand of 2,6-bis(3-pyrazolyl)pyridine: Synthesis, structure, surface photovoltage spectroscopy and photocatalytic activity

Ya Nan Hou[a], Zhi Nan Wang[a], Feng Ying Bai*[b], Qing Lin Guan[a], Xuan Wang[a], Rui Zhang[a] and Yong Heng Xing*[a]

[a] College of Chemistry and Chemical engineering, Liaoning Normal University, Huanghe Road 850#, Dalian City, 116029, P.R. China.

[b] College of Life Science, Liaoning Normal University, Dalian 11602, P.R. China

*e-mail: yhxing2000@yahoo.com

tel: 0411-82156987

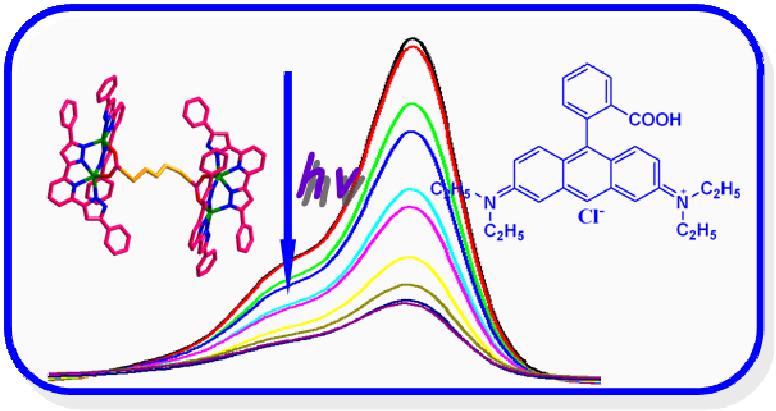

Text:

Synthesized three novel d^7/d^{10} metal complexes with N-heterocyclic ring ligand of 2,6-bis(3-pyrazolyl)pyridine firstly and studied the surface photovoltage spectra and photocatalytic activities.

Cite this: DOI: 10.1039/c0xx00000x

www.rsc.org/xxxxxx

ARTICLE TYPE

Three novel d^7/d^{10} metal complexes with N-heterocyclic ligand of 2,6-bis(3-pyrazolyl)pyridine: Synthesis, structure, surface photovoltage spectroscopy and photocatalytic activity

Ya Nan Hou[a], Zhi Nan Wang[a], Feng Ying Bai*[b], Qing Lin Guan[a], Xuan Wang[a], Rui Zhang[a] and Yong Heng Xing*[a]

Received (in XXX, XXX) Xth XXXXXXXXX 20XX, Accepted Xth XXXXXXXXX 20XX
DOI: 10.1039/b000000x

By introduction of different spanning flexible dicarboxylate acid as a second organic ligand, three complexes **$[Co_2(\mu_2\text{-ox})(H_2L)_2(HCOO)_2]$ (1)**, **$[Co_2(\mu_4\text{-ad})_{0.5}(HL)_2]\cdot(OH)\cdot(H_2O)$ (2)**, **$[Zn_2(\mu_4\text{-sub})_{0.5}(HL)_2]\cdot(OH)\cdot(H_2O)$ (3)** (H_2L=2, 6-di-(5-phenyl-1H-pyrazol-3-yl)pyridine, ox= oxalic acid, ad= adipic acid, sub= suberic acid) were synthesized by hydrothermal method. All the complexes were characterized by elemental analysis, IR and UV-vis spectroscopy and single-crystal X-ray diffraction. Structural analysis reveals that in complex **1**, Co(II) atom was six-coordinated to form a distorted octahedron while in complexes **2** and **3**, Co(II) and Zn(II) atom were five-coordinated to form disordered tetragonal coordination geometries. Acting as a bridge, flexible dicarboxylate in complex **1** coordinated with two metal atoms while in complexes **2** and **3** coordinated with four metal atoms. The surface photovoltage spectroscopy and photocatalytic activities of complexes **1**, **2** and **3** were also investigated in detail.

Introduction

Pyrazole derivatives are an important family of organic photochromic compounds and draw vigorously attention of chemical researchers especially in the field of metal- organic complexes synthesis over the several past decades[1]. Among these derivatives, pyridine-based tridentate compounds are very interesting polydentate N-heterocyclic ligands for coordination chemistry (Figure.1)[2]. So it is necessary to do a great deal of work to extend the knowledge of relevant structural types and establish proper synthetic strategies to design desirable architectures with physical properties[3]. Regarding pyrazole derivatives as an polydentate heterocyclic ligand is based on the following consideration: (i) the N atom of pyridine ring and two adjacent N atoms of the other two pyrazole rings could coordinate with metal atoms more easily and form stable tridentate complexes and the two rest N atoms of the two pyrazole rings could coordinate with other metal atoms to form a binuclear even tetranuclear and some more complicated complexes[4], for example, $[\{Co(H_2L)_2\}(H_2L)_4][PF_6]_2$ (H_2L=2,6-bis(5-phenylpyrazol-3-yl)-pyridine)[5], $[Fe_6(bpp)_4(\mu_3\text{-}O)_2(\mu\text{-}OMe)_3(\mu\text{-}OH)Cl_2]$ (H_2bpp=2,6-bis(pyrazol-3-yl)pyridine)[6], $[Cd_2(\mu\text{-}Tab)_2(Tab)_2(bdmppy)]_2(PF_6)_8\cdot H_2O$ (TabH = 4-(trimethylammonio)benzenethiol, bdmppy=2,6-bis(3,5-dimethyl-1*H*-pyrazol-1-yl)pyridine) [3e]; (ii) there is a tautomeric equilibrium of the bis-pyrazole compound in solution and the H atom of pyrazolyl NH can transfer to the adjacent N atoms[7]. Namely, the ligand might loose one H atom on the pyrazole ring, two H atoms of two pyrazole rings or loose no H atom according to the oxidation state of the metal atoms and the other ligands composed in the complex. (iii) it is commercially available or straightforward to synthesize and (iv) particularly those substituted at the 3, 4, 5-position on pyrazolyl moiety, are also readily accessible. Further more, if these positions were substituted by phenyl rings or pyridine rings, it is easy to form a bulky conjugating system. Complexes based on these kinds of ligands which possess bulky conjugating system present well properties on photoluminescence and photoelectric effect on the surface. By the ideas mentioned above, recently, we have successfully synthesized a series of complexes with pyridine-based pyrazole derivatives as ligands, 2, 6-di-(5-phenyl-1H-pyrazol-3-yl)pyridine and 2, 6-di-(5-methyl-1H-pyrazol-3-yl)pyridine (Figure.2) [3a, 8]. These two kinds of ligands commonly exhibit two kinds of coordination modes: quadridentate coordination mode: $\mu_4\text{-}\eta^1\text{-}\eta^1\text{-}\eta^1\text{-}\eta^1$ and trident chelate coordination mode[2b, 9].

On the other hand, dicarboxylic acid have been also widely used as ligands in metal coordination chemistry for their possessing interesting features, main virtue: (i) the presence of two carboxylate groups capable of bidentate and monodentate linking modes with terminal or bridging ligand; (ii) the possibility to obtain mono- or di-anionic forms; (iii) the probability of carboxylate triply coordination and (iv) the possibility to form secondary building blocks[10]. To our knowledge, although an amount of metal coordination polymers with the rigid (R) and flexible (F) dicarboxylate were reported[11], N-heterocyclic-transition metal complexes with different spanning flexible (F) dicarboxylate as an auxiliary ligand have been reported rarely.

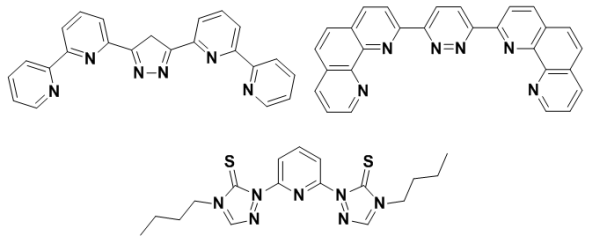

Figure.1 Pyridine-based tridentate ($\widehat{NN}$ N $\widehat{NN}$) N-heterocyclic

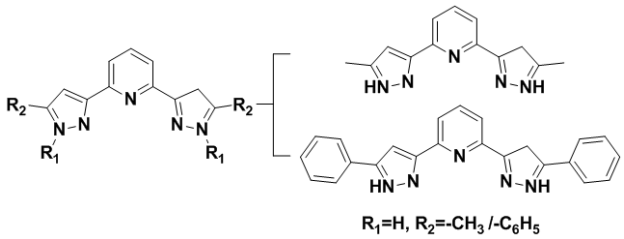

Figure.2 Structure of 2, 6-di-(5-phenyl-1H-pyrazol-3-yl)-pyridine and 2,6-di-(5-methyl-1H-pyrazol-3-yl)pyridine

Complexes based on these pyridine-based pyrazole derivatives had been applied in many fields, for example: the catalytic transfer hydrogenation of ketones[12], homogeneous catalysis[13], biological activity[14], etc., in particular, the ligands synthesized by us possess bulky conjugating system formed by one pyridine ring and two pyrazole rings, it made them widely researched in the field of photochromic material. However, study about photoelectric effect on the surface and photocatalytic activity of this kind of complexes had been rarely reported[15]. In this paper, we synthesized three transition-metalic complexes $[Co_2(\mu_2\text{-}C_2O_4)(H_2L)_2(HCOO)_2]$ **(1)**, $[Co_2(\mu_4\text{-ad})_{0.5}(HL)_2]\cdot(OH)\cdot(H_2O)$ **(2)**, $[Zn_2(\mu_4\text{-su})_{0.5}(HL)_2]\cdot(OH)\cdot(H_2O)$ **(3)** firstly with H_2L ligands and preformed studies of the structure, IR spectra, UV-vis spectra, photoluminescent properties. The surface photovoltage spectra and photocatalytic activity of the three complexes were also investigated in detail.

Experimental Section

General Considerations

H_2L were synthesized according to the modified literature method (Scheme.S1)[16]. A 30 % aqueous solution of hydrogen peroxide was used as primary oxidant. All other chemicals purchased were of reagent grade or better and used without further purification. IR spectra were recorded on a JASCO FT/IR-480 PLUS Fourier Transform spectrometer with pressed KBr pellets in the range 200–4000 cm^{-1}. The elemental analyses for C, H, and N were carried out on a Perkin Elmer 240C automatic analyzer. The luminescence spectra were reported on a JASCO F-6500 spectrofluorimeter (solid). UV–vis absorption spectra diffuse reflection was recorded with a JASCO V–570-UV/VIS/NIR spectrophotometer in the 200–2500 nm. Surface photovoltage spectroscopy (SPS) and field-induced surface photovoltage spectroscopy (FISPS) measurements were conducted on the sample in a sandwich cell (ITO/sample/ITO) with the light source-monochromator-lock-in detection technique[17]. Standard *p*-typed silicon flake is used to adjust comparative phase and xenon lamp is used as an illuminant to supply a radiation in the range of 300-800 nm.

Synthesis

$Co_2(\mu_2\text{-ox})(H_2L)_2(HCOO)_2$ (1). A mixture of $CoCl_2\cdot6H_2O$ (0.2 mmol, 47.6 mg), H_2L (0.2 mmol, 72.6 mg), oxalic acid (0.2 mmol, 18.0 mg), DMF (5 mL) and water (10 mL) was stirred for 3 h at room temperature. The diisopropylanmine was added dropwise until the pH=5.0 during stirring. Then, the mixture was transferred to a 20mL Teflon reactor and kept at 160 ºC for 3 days under autogenous pressure. It was cooled down to room temperature at 10 ºC /h. Orange block-like single crystals (yield: 55% based on Co) were obtained after filtration and washing with distilled water. Anal. Calc. for $C_{50}H_{36}N_{10}O_8Co_2$ (1022.75): C, 58.72; H, 3.55; N, 13.70. Found: C, 58.61; H, 3.44; N, 13.88%. IR data (KBr, cm^{-1}): 3441(vs), 3135(w), 3101(w), 3062(w), 2969(w), 2926(w), 2854(w), 1642(vs), 1598(vs), 1453(s), 1376(w), 1310(s), 1050(w), 1014(w), 981(w), 915(w), 800(w), 762(s), 685(w). UV-vis data (λ_{max}, nm): 208, 254, 330, 420, 544, 704, 1158.

$[Co_2(\mu_4\text{-ad})_{0.5}(HL)_2]\cdot(OH)\cdot(H_2O)$ (2). Complex **2** was prepared in the same manner as it described for **1** except that oxalic acid was replaced by adipic acid (0.2 mmol, 29.2 mg). The pH value was adjusted to 6.0 with diisopropylanmine. Orange block-like crystals of **2** were obtained in a yield of 58% based on Co(II). Anal. Calc. for $C_{49}H_{39}N_{10}O_4Co_2$ (949.76): C,61.97; H, 4.14; N, 14.75. Found: C, 62.02; H, 4.11; N, 14.55%. IR data (KBr, cm^{-1}): 3441(vs), 3062(w), 2962(w), 2926(w), 2854(w), 1606(vs), 1574(vs), 1453(vs), 1423(s), 1324(w), 1286(s), 1201(w), 1157(w), 1113(w), 1077(w), 1017(s), 967(w), 915(w), 806(w), 789(w), 762(vs), 693(s). UV-vis data (λ_{max}, nm): 222, 268, 340, 506, 684, 1156.

$[Zn_2(\mu_4\text{-sub})_{0.5}(HL)_2]\cdot(OH)\cdot(H_2O)$ (3). $ZnAc_2\cdot2H_2O$ (0.2 mmol, 43.9 mg),H_2L (0.2 mmol, 72.6 mg), suberic acid (0.2 mmol, 34.8 mg), DMF (3 mL) and H_2O (10 mL) were mixed in a 25 mL beaker and stirred. The pH value was adjusted to 6.0 with diisopropylanmine. After being stirred for 3 h at room temperature, the final mixture was sealed in a 25mL Teflon-lined stainless steel vessel and heated at 180 ºC under autogenous pressure for 3 days. The reactor was subsequently cooled down to room temperature at a rate of 10ºC/h. Colorless block-like crystals(yield: 51% based on Zn) suitable for X-ray diffraction were obtained after filtration and washing with distilled water. Anal. Calc. for $C_{50}H_{41}N_{10}O_4\ Zn_2$(949.76): C, 61.49; H, 4.23; N, 14.34. Found: C, 61.60; H, 4.44; N, 14.15%. IR data (KBr, cm^{-1}): 3441(vs), 3062(w), 2923(w), 2827(w), 1615(vs), 1576(vs), 1456(vs), 1286(w), 1157(w), 1113(w), 1077(w), 1020(s), 967(w), 915(w), 762(s), 693(s). UV-vis data (λ_{max}, nm): 266, 368, 418.

X-ray Crystallographic Determination

Suitable single crystals of four compounds were mounted on glass fibers for X–ray measurement. Reflection data were collected at room temperature on a Bruker AXS SMART APEX II CCD diffractometer with graphite monochromatized Mo Kα radiation (λ=0.71073 Å). All the measured independent reflections ($I > 2\sigma(I)$) were used in the structural analyses, and semi-empirical absorption corrections were applied using SADABS program[18]. Crystal structures were solved by the direct method. All non-hydrogen atoms were refined anisotropically. Hydrogen atoms on carbon and nitrogen were fixed at calculated positions and refined by using a riding model. The Hydrogen

atom of coordination water and lattice water molecules were found in difference Fourier map. All calculations were performed using the SHELX–97 program[19]. For **3**, C47-C54 of the suberic acid ligand were disordered over two positions with the site occupancy factors of 0.50/0.50. Crystal data and details of the data collection and the structure refinement are given in Table.1. The selected bond lengths and angles around metal atom of complexes **1–3** are listed in Table.S1.

Table 1 Crystallographic Data for Complexes **1–3***

Complex	**1**	**2**	**3**
Formula	$C_{50}H_{36}N_{10}O_8Co_2$	$C_{49}H_{39}N_{10}O_4Co_2$	$C_{50}H_{41}N_{10}O_4Zn_2$
M (g mol–1)	1022.75	949.76	976.67
Crystal system	Monoclinic	Triclinic	Triclinic
Space group	Cc	P-1	P-1
a (Å)	32.762(7)	11.396(2)	10.941(2)
b (Å)	10.724(2)	15.014(3)	12.616(3)
c (Å)	13.937(3)	15.094(3)	17.363(4)
α (deg)	90	72.47(3)	105.61(3)
β (deg)	114.43(3)	84.22(3)	102.34(3)
γ (deg)	90	81.61(3)	90.47(3)
V (Å3)	4457.9(15)	2431.8(8)	2249.5(8)
Z	4	2	2
Dcalc (g cm-3)	1.524	1.297	1.442
F(000)	2096	978	1006
μ(Mo-Kα)/mm^{-1}	0.814	0.735	1.124
θ (deg)	3.21- 27.48	3.09 -27.48	3.25 - 25.35
Reflections collected	20916	23324	18402
Independent reflections(I >2σ)	9063(3844)	10823(6272)	8180(4139)
Parameters	631	585	633
Δ(ρ) (e Å–3)	0.319 and -0.326	1.294 and -0.924	1.639 and -0.561
Goodness of fit	0.985	1.055	0.956
R^a	0.0698(0.1862)	0.0863 (0.1403)	0.0891(0.1674)
$wR2^b$	0.1162(0.1502)	0.2504 (0.2919)	0.2363(0.2902)

* $^aR = \Sigma||Fo|-|Fc||/\Sigma|Fo|$, $wR_2 = [\Sigma(w(Fo^2-Fc^2)^2/\Sigma(w(Fo^2)^2)]^{1/2}$; [$Fo > 4\sigma(Fo)$]; ^{b}based on all data.

Results and Discussion

Synthesis

The three complexes were syththesized by the reaction of transition metal salts ($CoCl_2{\cdot}6H_2O$ and $ZnAc_2{\cdot}2H_2O$), H_2L ligand

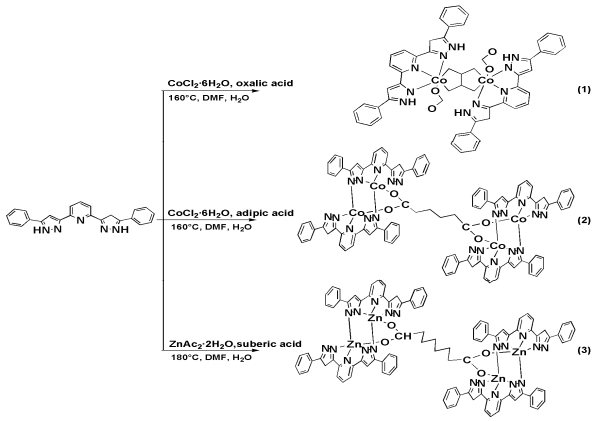

Scheme.1 The reaction process of complex **1-3**

and different spanning dicarboxylate (oxalic acid, adipic acid and suberic acid) with the molar ratio of 1:1:1 under hydrothermal conduction (Scheme.1). During the prosess of these experiments, it is found that the mixed solution of H_2O and DMF is better to crystal growth than that of H_2O and EtOH. The crystal of the corresponding complexes were successfully obtained when we ajusted the pH value of the solution to 5 or 6, hence, the pH value of the solution is a very sensitive reaction parameter. It worth to mention that the formyl anion in the structure of complex **1** may be produced by DMF hydrolysis in the reaction course. It may be due to the DMF can hydrolysis at a weak acid condition (pH=5)[20].

Additionally, powder X-ray diffraction (PXRD) for the complexes **1**, **2** and **3** was used to confirm the phase purity of the bulk samples. As shown in Figure.S1-S3, all the peaks presented in the measured patterns closely match in the simulated patterns generated from single crystal diffraction data.

Structural analysis of complexes 1-3

$Co_2(\mu_2\text{-ox})(H_2L)_2(HCOO)_2$ (1). Complex **1** is crystallized in the Monoclinic system with *Cc* space group. X-ray single crystal analysis indicates that the asymmetric unit of the complex **1** (Figure.3a) is made up of two Co(II) atoms, two H_2L ligands, one bridging oxalate ligand and two $HCOO^-$ groups. Co1 coordinated with three nitrogen atoms (N7, N8, N9) from H_2L ligand, two oxygen atoms (O3, O4) from an oxalate group, one oxygen atom (O2) from $HCOO^-$ group to form a distorted octahedron. Co2 adopted the same coordinate mode as Co1. In the molecular structure, N7, N8, N9, O4 and N2, N3, N4, O5 were in the equatorial plane, O2, O3 and O6, O7 were in the axial positions, respectively. The two metal atoms were linked by the bridging oxalate ligand with the contact of 5.44 Å. Bond length of Co-O_{carb} ranged from 2.001 to 2.100 Å. The length of Co-N_{pz} was in the range of 2.139 to 2.276 Å and the length of Co-N_{py} was 2.057 and 2.139 Å. The angles of O-Co-O, N-Co-N and N-Co-O vary from 78.8(4) to 90.1(4)°, 73.6(5) to 75.7(5)°and 83.9(5) to 109.4(5)°, respectively.

In the structure of the complex **1**, H_2L ligand is coordinated with Co atom by the tridentate coordination mode with $\mu_1{-}\eta^1{-}\eta^1{-}\eta^1$ chelating fashion, namely, two N atoms from two pyrazolyl rings, one N atom from one pyridine ring. However, for oxalate ligand, it presents a $\mu_2{-}\eta^1{-}\eta^1{-}\eta^1{-}\eta^1$ bridging

coordination mode, and the $HCOO^-$ group exhibits a terminal coordination mode. The adjacent Co atoms were connected by a bridging oxalate ligand to form a binuclear [Co–2,6-di(5-phenyl-1H-pyrazol-3-yl)pyridine]-oxalate-[Co-2,6-di(5-phenyl-1H-pyrazol-3-yl)pyridine] complex. Pyrazolyl rings from two sides are distorted to the least-squares plane (central pyridyl ring) with dihedral angle varying from 1.25(1.15) to 13.89(1.16)°.

There are three kinds of hydrogen bonds in complex **1**: (Ⅰ) C—H···O type between the carbon atom (donor) from H_2L and oxygen (acceptor) from $HCOO^-$ group; (Ⅱ) N—H···O type between the nitrugen atom (donor) from H_2L and oxygen (acceptor) from $HCOO^-$; (□) C—H···O type between the carbon atom (donor) from H_2L and oxygen (acceptor) from oxalate group. By hydrogen bonding of (□) and (□), adjacent molecular unit were connected (Figure.3b) to form an infinite supramolecular chain (Figure.3c) like a zigzag. Furthermore, two adjacent chains were furthermore linked via hydrogen bonds (□) to form a 2D supramolecular network (Figure.3d). The detail data of hydrogen bonds was list in Table.2.

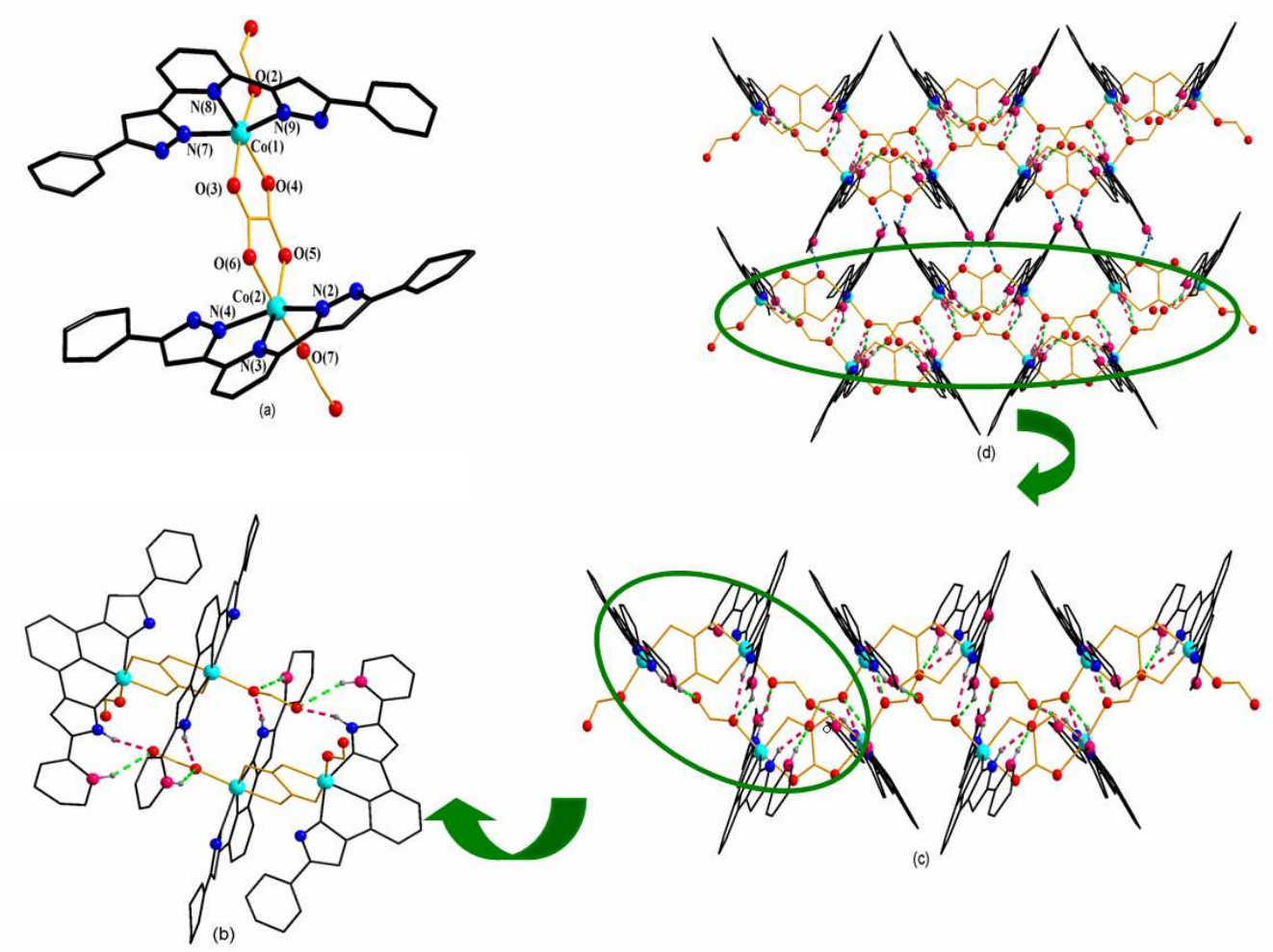

Figure.3 (a) The asymmetric unit of complex **1**; **(b)** Adjacent molecular unit were connected by hydrogen bonding of (Ⅰ) and (Ⅱ); **(c)** The zigzag infinite supramolecular chain connected by hydrogen bonding of (Ⅰ) and (Ⅱ); **(d)** The 2D supramolecular network connected by hydrogen bonding of (Ⅲ); (The green line represent the hydrogen bonding of (Ⅰ); the pink line represent the hydrogen bonding of (Ⅱ) and the blue line represent the hydrogen bonding of (Ⅲ)).

Cite this: DOI: 10.1039/c0xx00000x

www.rsc.org/xxxxxx

ARTICLE TYPE

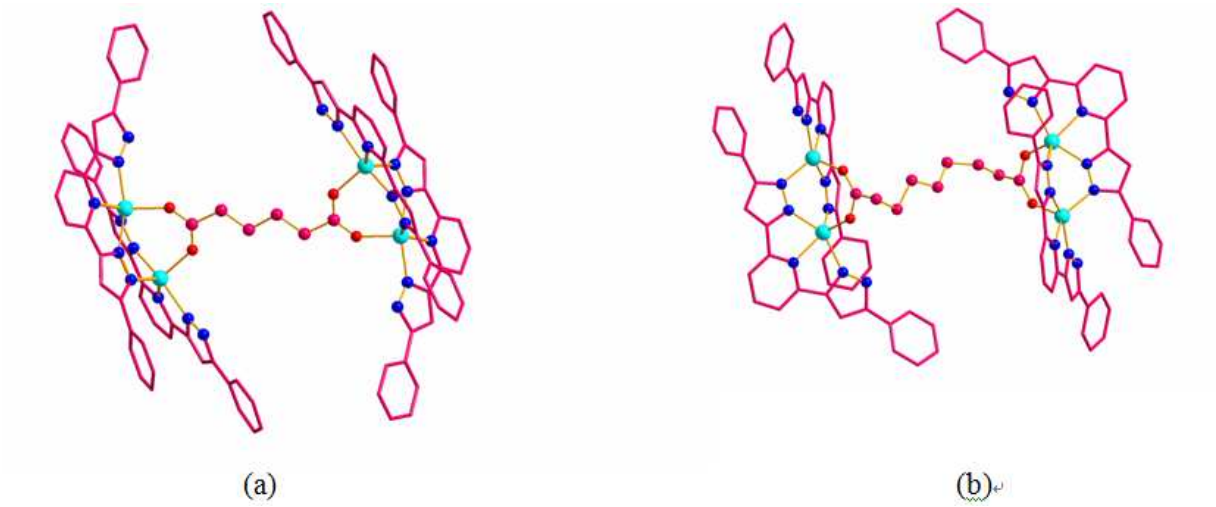

Figure.4 (a) The molecular structure of complex **2**; **(b)** The molecular structure of complex **3**. (The lattice water molecular and OH^- group in Figure.4 were all deleted.)

$[Co_2(\mu_4\text{-ad})_{0.5}(HL)_2]\cdot(OH)\cdot(H_2O)$ (2) and $[Zn_2(\mu_4\text{-sub})_{0.5}(HL)_2]\cdot(OH)\cdot(H_2O)$ (3). The single-crystal X-ray analysis reveals that the complex **2** is crystallized in the triclinic system with space group *P-1*. There existed two Co(II) center, two H_2L ligands, an half bridging adipic acid, one lattice water molecular and one lattice OH^- group in the asymmetric unit of **2** (Figure.4a). Co1 was five-coordinated by four nitrogen atoms (N2, N3, N4, N10) from two H_2L ligands, in which N2, N3 and N4 belong to one H_2L ligand while N10 comes from pyrazole ring of another H_2L ligand and one oxygen atom (O2) from the adipic acid ligand to generate a disordered tetragonal pyramid coordination geometry. The coordination environment of Co2 was similar to that of Co1. Co1 and Co2 were connected by four nitrogen atoms (N4, N5, N9 and N10) from two pyrazolyl rings of two H_2L ligands and one

Table 2 Bond Distances (Å) and Angles (°) of Hydrogen Bonds in Complexes **1-3***

D-H···A	d (D-H) Å	d (H···A) Å	d (D···A) Å	∠DHA(°)
Complex **1**				
N 1-H1A···O2$^{\#1}$	0.8600	1.8700	2.7227	170.00
N 5-H5A···O8$^{\#2}$	0.8600	1.9300	2.7466	157.00
N 6-H6A ···O7$^{\#2}$	0.8600	2.0200	2.8638	165.00
N10-H10A···O1$^{\#1}$	0.8600	1.9200	2.7140	152.00
C11-H11A···O3$^{\#3}$	0.9300	2.3600	3.2299	155.00
C23-H23···O8$^{\#2}$	0.9300	2.2500	3.1418	160.00
C34-H34···O6$^{\#4}$	0.9300	2.3600	3.1891	148.00
Complex **2**				
N1-H1A···O1W	0.8600	1.9800	2.778	154.00
N6-H6A···O3W$^{\#5}$	0.8600	1.9400	2.771	162.00
Complex **3**				
N6-H6A···O1W	0.8600	2.5200	3.120	127.00
N6-H6A···O2W	0.8600	1.8800	2.73	166.00

*Symmetry transformation used to generate equivalent atoms: #1: x, 1-y, 0.5+z; #2: x, 1-y, -0.5+z; #3: x, -y, 0.5+z; #4: x, -y, -0.5+z; #5: 1-x, 1-y, 1-z; #6: 1- x, 1-y, 1-z.

carboxylate group of adipic acid to form a mixed three-bridging binuclear unit which furthermore stabilize the structure of complex **2**. In the molecular structure of complex **2** (Figure.4b), the H_2L ligand adopted the $\mu_2\text{-}\eta_N^1\text{-}\eta_N^1\text{-}\eta_N^1\text{-}\eta_N^1$ coordination fashion, and the adipic acid adopted a $\mu_4\text{-}\eta_O^1\text{-}\eta_O^1\text{-}\eta_O^1\text{-}\eta_O^1$ coordination fashion. The contact between Co1 and Co2 in the binuclear unit is 3.6197 Å, and the contact between Co1 and Co1, which linked by the adipic acid ligand is 12.4437 Å while that of Co2 and Co2 is 10.9699 Å.

The single-crystal X-ray analysis reveals that complex **3** is also crystallized in the triclinic system with *P-1* space group as the same as complex **2**. The structure of complex **3** is similar to that of the complex **2,** and the only difference is that central metal of Co atoms and longer dicarboxylate ligand (adipic acid) were replaced by Zn atom and suberic acid ligand, respectively. The asymmetric unit of **3** (Figure.4c) is completed by two Zn atoms, two HL_2 ligands, a half suberic acid ligand, one lattice formic acid molecule and one lattice water molecule. The coordination environments of zinc atoms are shown in Figure.4c. Zn (II) is five-coordinated by four N atoms (N2, N3, N4, N10 for Zn1; N5, N7, N8, N9 for Zn2 from two $(HL^2)^-$ ligand with Zn-N bond lengths in the range of 1.983~2.210 Å, one oxygen atoms (O1 for Zn1; O2 for Zn2) from one subric acid ligand with Zn-O bond length of 1.988 and 2.002 Å, to form a distorted tetrahedral geometry, which is best described by the structural parameter τ=0.308 for Zn1 and 0.255 for Zn2[21]. The angles of O-Zn-N and N-Zn-N are in the range of 94.72(11)~124.23(11)^o and 73.97(11)~148.80 (11)^o, respectively. Pyrazolyl rings from two

sides are distorted to the least-squares plane (central pyridyl ring) with dihedral angle varying from 0.81(0.61) to 3.85(0.38)°. In the molecular structure of the complex **3** (Figure.4d), flexible suberic acid ligand in the complex **3** is in the form of μ_4-bridging coordination fashion with each side carboxylate group in μ_2–η^1–η^1 monodentate mode to bridge linking two adjacent Zn atoms to form a tetra-nuclear discrete Zn-HL_2-Sub complex. The adjacent Zn atoms were connected by three different bridging groups from two $(HL^2)^-$ ligands and one carboxylate group of sub^{2-} ligand with Zn1---Zn2 contact of 3.68 Å, to form a building unit of $Zn_2(HL_2)_2$. The $Zn_2(HL_2)_2$ building unit is further linked by the flexible sub^{2-} ligand with Zn1---Zn1 contact of 12.02 Å and Zn2---Zn2 contact of 12.432 Å.

Structural comparison of complex 1-3. The comparison of structure in the complexes **1-3** found that although the molecular structures of **1-3** included the same N-heterocyclic ligands, 2,6-di(5-phenyl-1H-pyrazol-3-yl)pyridine, the coordination mode in complex **1** is different from those of the complexes **2**-**3**. H_2L acts as a pincer tridentate chelate fashion of μ_1–η^1–η^1–η^1 for complex **1**, while H_2L acts as a tetradentate chelate fashion, which adopts a μ_2–η^1–η^1–η^1–η^1 coordination fashion in complex **2** and **3**.

The order of the corresponding bond lengths of M-N are M-$N_{pyridine}$ < M-$N_{pyrazolyl}$ for the complexes **1-3**. In addition, pyrazolyl rings from two sides are distorted to the least-squares plane (central pyridine ring) with the different dihedral angles in the range of 0.81(0.61) to 13.89(1.16) °. This may be led by the different spanning dicarboxylate ligands and their various coordination modes.

On the other hand, the comparison of the dicarboxylic acid ligands on the influence of the structures from the complexes **1-3** found that the coordination modes of the dicarboxylic ligands are also different. For ox^{2-} ligand in the complex **1**, ox^{2-} ligand presents a μ_2–η^1–η^1–η^1–η^1 bridging coordination mode linking two Co atoms; the carboxylate group of the ad^{2-} ligand in the complex **2** adopts a μ_4–η^1–η^1–η^1–η^1 bridging coordination mode to link four Co atoms. The coordination fashion of the suberic acid ligand in the complex **3** is the same as that of the ad^{2-} ligand. The bonds length of the M-$O_{carboxylate}$ in complex **1** is longer than those of complexes **2** and **3**, and the bond length of M-$O_{carboxylate}$ of the complex **2** is slightly longer than that of the complex **3**. This phenomenon could be also attributed to the different coordination modes of the different spanning dicarboxylate ligands in the three complexes.

IR spectra

For IR spectra of complex **1** (Figure.S4), a broad absorption band appearing at 3439 cm^{-1} indicates the stretching vibrations of the N-H on the pyrazolyl rings and pyridine rings. A weak peak at 3137 cm^{-1} should be assigned to the stretching vibrations of the Ar-H on the phenyl rings. A weak peak appears at 3061 cm^{-1} because of the C-H stretching vibrations of the pyridine/pyrazolyl rings. The bands at 1598 cm^{-1} and 1310 cm^{-1} are attributed to the symmetrical stretching vibration and asymmetrical stretching vibration of C=O bond, respectively. Absorptions at 1644 and 1448 cm^{-1} are the characterization of stretching vibration of C=C or C=N on the phenyl and pyridine rings. The characteristic bands (C-C, C-N) of pyrazholyl and pyridine rings appear at 808 cm^{-1}, 768 cm^{-1} and 1017 cm^{-1}. IR spectra of complexes **2** and **3** (Figure.S5 and Figure.S6) are similar to that of **1**. The detailed attributions of IR (cm^{-1}) for complex 1-3 are listed in Table S2.

UV–vis spectra

The electronic absorption spectra of complexes **1-3** are shown in Figure.5. Bands at 254 nm for **1**, 268 nm for **2**, 266 nm for **3** are attributed to the π–π* transition of the ligands. It is found that the π–π* transition move slightly to blue–shift by a comparison with the π–π* transition of H_2L. Bands at 330 nm and 420 nm for **1**, 340 nm for **2**, 368 nm and 418 nm for **3** are due to the LLCT (inter-ligand charge transfer transition). Broad peaks at 544 nm and 1158 nm for **1**, 506 nm 684 nm and 1156 nm for **2** should be caused by the d-d* transition of Co(□)[22]. It reveals that the absorption band for **2** more slightly red-shift than that of **1**, this phenomenon might be caused by the different coordinate modes of the ligands (H_2L, oxalic acid and adipic acid).

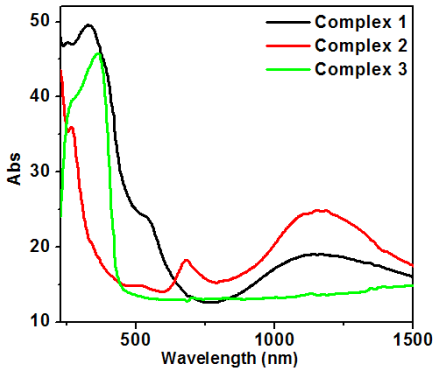

Figure.5 The UV-vis spectra of complex **1-3** in the form of solid state.

Photoluminescence

Photoluminescence examination of the Zn-containing compound **3**, with typical d^{10} transition-metal configuration, was examined at room temperature with solid state. As shown in Figure.6, a broad luminescence band at 415 nm was detected in the emission spectrum when it was excited at 365 nm. However, the free H_2L ligand shows a strong emission band at 357 nm with an excitation of 337 nm. Accordingly, the emission peak of **3** should be attributed to the metal-to-ligand charge-transfer (MLCT) transition[23].

Photovoltage Surface Spectra

Surface photovoltage (SPV) is the most ordinary and the most sensitive method to study the photo-electricity property. The character of photovoltaic response of organic semiconductor, inorganic semiconductor, organic/inorganic semiconductor and the transition or diffusion of electron on the surface of solid sample could be detected via SPV[24], it could be performed by the surface photovoltage spectroscopy (SPS). Surface photovoltage spectroscopy (SPS) is an effective technique to investigate the surface charge behavior of solid sample. SPS is a well-established contactless technique for the characterization of semiconductor materials, which relies on analyzing illumination-induced changes in the surface voltage. The studies had begun in the late 1940s and after several decades of research, SPS had

become a high sensitive tool to detect the change of surface electronic behaviors by the reason of celerity, facility and without breakage[24, 25]. It is significant for research on electronic transition of surface and interface because it not only related to the electronic transition under light–induced, but also reflected the separation and diversion of photo–generated charge. At present, SPV has been employed in the studies of charge transfer in photo–stimulated surface interactions, dye sensitization processes, photo–catalysis electronic, and charge transition between different phase, surface electronic behaviors and photo–electric conversation. By studying SPS of the sample, we can not only know the electron transition behavior on surface but also make a

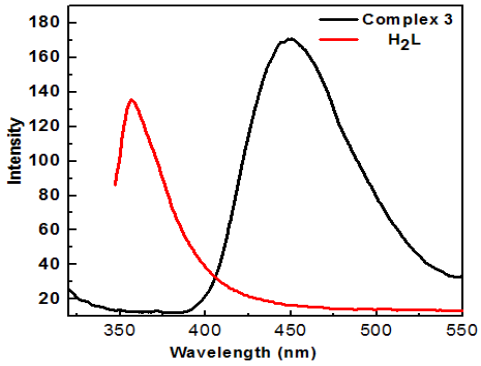

Figure.6 The photoluminescence spectra of H_2L ligand and complex **3**. For complex **3**, a broad luminescence band at 450 nm was detected in the emission spectrum when it was excited at 365 nm. However, the free H_2L ligand shows a strong emission band at 357 nm with an excitation of 337 nm.

judgement of the type of a semiconductor sample. In SPS, the detected signal is equivalent to the change in the surface potential barrier on illumination (δVs). The value is calculated by the equation: $\delta Vs = Vs - V^0s$, which Vs and V^0s are the surface potential barriers before and after illumination, respectively. Positive response of SPV ($\delta Vs > 0$) means that the sample is characterized as a *p*–typed semiconductor, whereas the negative one means the sample is an *n*–typed semiconductor[17].

By analysis the UV-vis spectra of the three complexes, we could regard the three compounds as an extended semiconductor. In this paper, we could combine energy-band theory with crystal-field theory to explain the signals of SPS. The central metal atoms of the three compounds coordinated with O atoms or N atoms directly, we can take the multiple 2s 2p orbitals of O atoms and N atoms as the valence band and 4s 4p empty orbitals of Zn^{2+} or Co^{2+} ions as the conduction band. The empty d orbitals of central metal ions could be regarded as the impurity, which is in region of the valence bond and conduction band[26]. The SPS of complex **1**, **2** and **3** were shown in Figure.7(a), Figure.7(b) and Figure.7(c), some overlapping of signals was fixed after treating by Origin7.0 program. In complex **1**, the peak at 326 nm was attributed to LLCT and the peak at 388 nm was attributed to LMCT of O→ Co and N→Co. The peak at 545 nm and broad band at 743 nm might be caused by d-d* transition. Being similar with complex **1**, there were also four peaks on range of 300-800 nm of complex **2**. The peak at 335 nm was attributed to LLCT, and a high peak of 396 nm might caused by LMCT O→Co and N→ Co. The d-d* transition caused the responses at 476 nm and 669 nm. However, in complex **3**, only two peaks presented in SPS, and they were caused by LLCT (361 nm) and LMCT (392 nm) of O→ Zn and N→ Zn respectively.

It is worth to say that, every response of the signals moved to red-shift more or less when compared with them corresponding signals in the UV-vis spectra, this phenomenon might be caused by the loss of energy in the process of energetic transition. Secondly, in complex **1**, the peak of LLCT is twice higher than that of LMCT while opposite phenomenon appeared in complexes **2** and **3**. By careful analysis and comparison of structures of the three compounds, reason caused this phenomenon should be attributed to the different coordinated types of the three compounds. In complex **1**, the central metal atom coordinated with three N atoms from one H_2L ligand.

However, in complexes **2** and **3**, the central atoms coordinated not only with three N atoms of one H_2L ligand but also another N atom from one pyrazole ring of another H_2L ligand to form a circular system of (metal atom)-ligand-(metal atom)-ligand which made it more effective of the electron transition between coordinated ligands and central metal atoms. Furthermore, for the three complexes, their absorption for the light range from 300 nm to 600 nm, this high utilization ratio made them behave extraordinary potential photoexcited materials.

Field-induced surface photovoltage spectroscopy (FISPS) is a means to adjudge the type of the semiconductor and it can be measured by applying an external electric field to the sample with a transparent electrode[27]. The intensity of the photovoltaic response signals was related to the efficiency of the separation of photoexcited electron–hole pairs and a positive electric field is beneficial to increase the efficiency whereas a negative one has the opposite effect. For a *p*-type semiconductor, when a positive electric field is applied on the semiconductor surface, the SPV response increases since the external field is consistent with the built-in field. On the contrary, when a negative electric field is applied, the SPV response is weakened. In contrast to *p*-type semiconductors, the SPV response intensity of *n*-type semiconductors increases as a negative field is applied and reduces as a positive electric field is applied[17]. The FISPS of complexes **1**, **2** and **3** was shown in Figure.8 (a, b, c). The intensities of the peaks all increase when the positive electronic (+0.2 V) field was applied, whereas, they reduced when the negative electronic field (-0.2 V) was applied. Hence, they behave the *p*-type semiconductor characteristic.

Photocatalytic Activity

The photocatalytic activities of complexes 1-3 were studied in detail. The rhodamine B (RhB) was selected as a model dye to evaluate the photocatalytic activities of degeneration the purification in the wastewater. A 18 W Hg lamp was used as thUV light source. The distance between the reaction vessel and the light source was 15 cm. During the process of the decomposing reaction, a UV251 spectrophotometer was used to monitor the reaction under the specific wavelength. To rule out the possibility that the photocatalytic activity of 1 and 2 arises from molecular or oligomeric species formed through dissolution of the solid samples in the photocatalytic reaction systems, controlled experiments were conducted. We filtered the reaction suspensions after 10 h of irradiation to remove the solid catalyst,

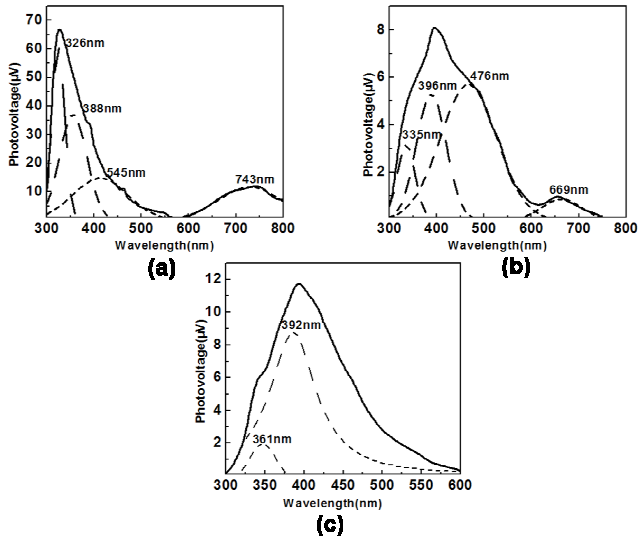

Figure.7 The SPS of complexes **1-3**.

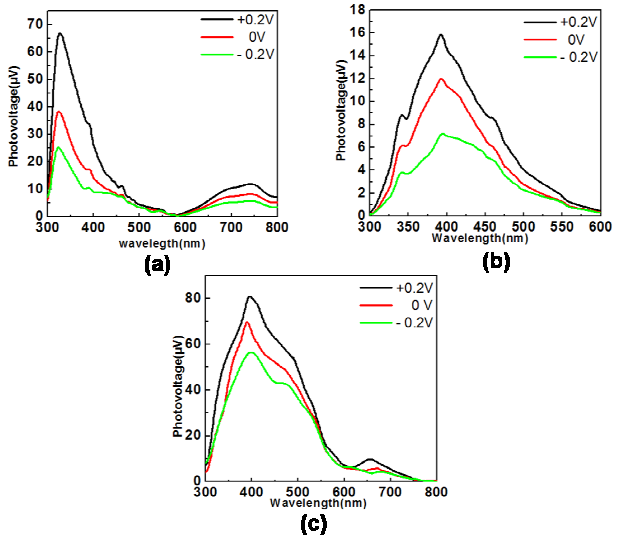

Figure.8 The FISPS of complexes **1-3**.

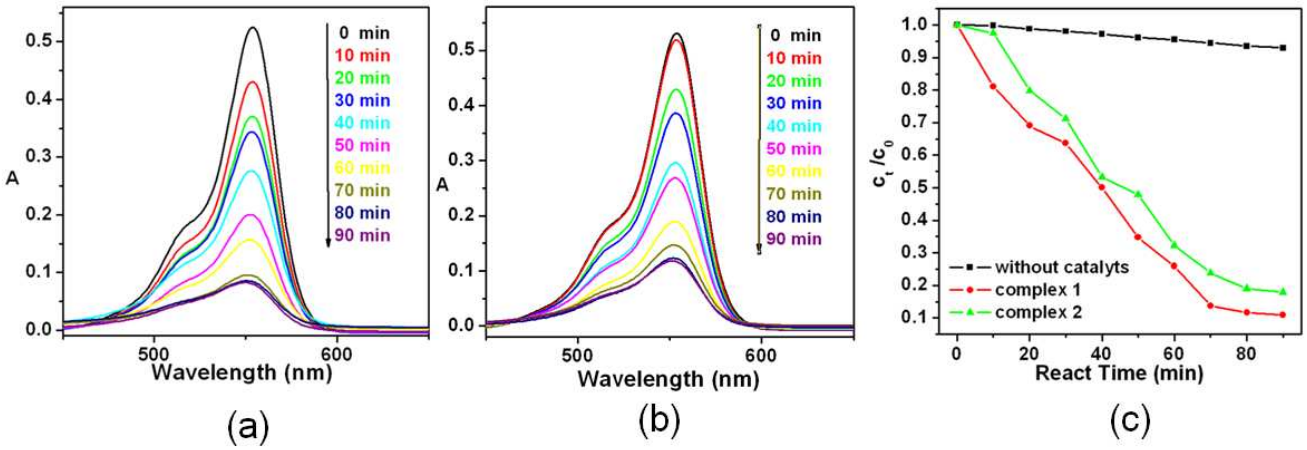

Figure.9 (a) The UV-vis absorption spectra of RhB solution during the reaction when complex **1** was used as catalyst; **(b)** The UV-vis absorption spectra of RhB solution during the reaction when complex **2** was used as catalyst; **(c)** Photocatalytic degradation of RhB solution.

and fresh RhB was added into the respective filtrates for catalysis testing.

Under the condition of the same temperature, intensity of the UV irradiation, concentration of the RhB solution and molar quantity of the catalysts, complexes **1-3** exhibited quite different photocatalytic activities under the UV irradiation. As it is shown in Figure.9, approximately 85% and 80% RhB was degenerated respectively in the absence of complexes **1** and **2**, the RhB solutions turned nearly colorless after about 70 min indicating that the degeneration process was almost completed. However, nearly no degenerating phenomenon was observed until 100 min when complex **3** was used as catalyst. To our knowledge, the photocatalytic effect of MOFs was mainly influenced by the central metals, the extent of the conjugation, the cooedinated environment, the structures of the complexes and the steric hindrance around the metal active centers etc.[28]. In this article, although the detail mechanism of the catalytic processes is still need to be carried on by doing further experiments, we still assumed that the cause of this phenomenon is the different central metals. During the photocatalytic process of complexes **1** and **2**, the highest occupied molecular orbital (HOMO) mainly comes from O and/or N 2p bonding orbitals (valence band) and the lowest unoccupied molecular orbital (LUMO) from empty Co orbitals (conduction band)[28e]. After irradiating by the UV light, one electron in the HOMO was excited to the LUMO. The one-electron-shorted HOMO then took one electron from H_2O molecule and lead to the formation of •OH active species which could furthermore complete the process of the photocatalytic degeneration. As to the different photocatalytic activities between complexes **1** and **2**, it might be caused by the different coordinated environments and structures of complexes **1** and **2**.

Conclusions

In this article, we synthesized three complexes using the 2,6-bis(3-pyrazolyl)pyridine as main ligands and dicarboxylate acid ligands with different spanning flexible chains as auxiliary ligands. Both of the three complexes were characterized by the single crystal X-ray diffraction analysis, elemental analysis and IR spectroscopy. The study of surface photovoltage spectra revealed that the three complexes all possessed well responses when the irradiation ranged from 300 nm to 800 nm. These well

responses made complexes **1-3** potential *p*-type semiconductors. As to the investigation of photocatalytic activity, the experimental results revealed that complexes **1** and **2** well photocatalytic property while nearly no degeneration occurred when complex **3** was used as catalyst. The different photocatalytic activities of complexes **1-3** were mainly caused by the metal centers Co(Ⅱ) and Zn(Ⅱ).

Acknowledgements

We are very thankful for the Program for the National Natural Science Foundation of China (Grant No.21371086).

Supporting information paragraph

Tables of atomic coordinates, isotropic thermal parameters, and complete bond distances and angles have been deposited with the Cambridge Crystallographic Data Center. Copies of this information may be obtained free of charge, by quoting the publication citation and deposition numbers CCDC 928253 **(1)** and 928254 **(2)** 928255 **(3)** from the Director, CCDC, 12 Union Road. Cambridge, CB2 1EZ, UK (fax+44-1223-336033; e-mail deposit@ccdc.cam.ac.uk; http://www.ccdc.cam.ac.uk).

Notes and references

[a] *College of Chemistry and Chemical engineering, Liaoning Normal University, Dalian, 116029, P.R. China. Fax: 86-0411-82156987; Tel: 86-0411-82156987. Corresponding author: Y. H. Xing; E-mail: yhxing2000@yahoo.com.*

[b] *College of Life Science, Liaoning Normal University, Dalian, 116029, P.R. China. Fax: 86-0411-82156987; Tel: 86-0411-82156987. Corresponding author: F. Y. Bai; E-mail: baifengying2000@163.com.*

† Electronic Supplementary Information (ESI) available: [The synthesise methods of H_2Lligands, IR spectra, PXRD]. See DOI: 10.1039/b000000x/

‡ Footnotes should appear here. These might include comments relevant to but not central to the matter under discussion, limited experimental and spectral data, and crystallographic data.

1 a)A.P. Sadimenko, S.S. Basson, *Coor. Chem. Rev*, 1996, **147**, 247; b) R. Mukherjee, *Coor. Chem. Rev*, 2000, **203**, 151; c) J. P. Zhang, S. Kitagawa, *J. Am. Chem. Soc*, 2008, **130**, 907; d) M. A. Halcrow, *Dalton Trans*, 2009, **12**, 2059.

2 a) B. Schneider, S. Demeshko, S. Dechert, F. Meyer, *Angew. Chem. Int. Ed*, 2010, **49**, 9274; b) T. D. Roberts, F. Tuna, T. L. Malkin, C. A. Kilnera, M. A. Halcrow, *Chem. Sci*, 2012, **3**, 349; c) J. I. van der Vlugt, S. Demeshko, S. Dechert, F. Meyer, *Inorg. Chem*, 2008, **47**, 1576.

3 a) Y. B. Zhou, W. Z. Chen, *Dalton Trans,* 2007, **44**, 5123; b) S. M. Hawxwell, L. Brammer, *CrystEngComm,* 2006, **8**, 473; c) L. Wang, Q. Yang, H. Chen, R. X. Li, *Inorg. Chem. Comm,* 2011, **14**, 1884; d) Y. B. Zhou, W. Z. Chen, D. Q. Wang, *Dalton Trans,* 2008, **11**, 1444; e) A. X. Zheng, H. F. Wang, C. N. Lu, Z. G. Ren, H. X. Li, J. P. Lang, *Dalton Tran.,* 2012, **41**, 558; f) B. Zhao, H. M. Shu, H. M. Hu, T. Qin, X. L. Chen, *J. Coor. Chem,* 2009, **62**, 1025; g) L. T. Ghoochany, S. Farsadpour, Y. Sun, W. R. Thiel, *Eur. J. Inorg. Chem,* 2011, **23**, 3431.

4 a) K. P. Rao, A. Thirumurugan, C. N. R. Rao, *Chem. Eur. J,* 2007, **13**, 3193; b) K. S. Banu, S. Mondal, A. Guha, S. Das, T. Chattopadhyay, E. Suresh, E. Zangrando, D. Das, *Polyhedron*, 2011, **30**, 163; c) M. A. Halcrow, *Coor. Chem Rev,* 2005, **249**, 2880.

5 T. R. Scicluna, B. H. Fraser, N. T. Gorham, J. G. MacLellan, M. Massi, *CrystEngComm,* 2012, **12**, 3422.

6 D. Plaul, E. T. Spielberg, W. Plass, *Z. Anorg. Allg. Chem,* 2010, **636**, 1268.

7 B. Zhao, H. M. Shu, H. M. Hu, T. Qin, X. L. Chen, *J.Coor. Chem*, 2009, **62**. 1025.

8 a) D. Rehder, G. Santoni, G. M. Licini, C. Schulzke, B. Meier, *Coor. Chem. Rev,* 2003, **237**, 53; b) M. Časný, D. Rehder, *Dalton Trans* 2004, **5**, 839; c) D. Rehder, *Inorg. Chem. Comm,* 2003, **6**, 604; d) M. T. Cocco, V. Onnis, G. Ponticelli, B. Meier, D. Rehder, E. Garribba, G. Micera, *J. Inorg. Biochem,* 2007, **101**, 19; e) P. Friedländer, *Ber. dtsch. chem. Ges*, 1909, **42**, 765.

9 a) S. Hu, Y. F. Zhao, H. M. Hu, L. Liu, *Acta Cryst*, 2011, **67**, 945; b) L. J. Wan, C. S. Zhang, Y. H. Xing, Z. Li, N. Xing, L. Y. Wan, H. Shan, *Inorg. Chem*, 2012, ***51* (12)**, 6517.

10 C. N. R. Rao, S. Natarajan, R. Vaidhyanathan, *Angew. Chem. Int. Ed*, 2004, **43**, 1466.

11 a) K. L. Hou, F. Y. Bai, Y. H. Xing, J. L. Wang, Z. Shi, *CrystEngComm,* 2011, **13**, 3884; b) Z. Wang, Y. H. Xing, C. G. Wang, L. X. Sun, J. Zhang, M. F. Ge, S. Y. Niu, *CrystEngComm*, 2010, **12**, 762; c) C. G. Wang, Y. H. Xing, Z. P. Li, J. Li, X. Q. Zeng, M. F. Ge, S. Y. Niu, *Cryst. Growth Des,* 2009, **9(3)**, 1525.

12 a) G. Zassinovich, G. Mestroni, S. Gladiali, *Chem. Rev,*1992, **91**,1051; b) S. Gladiali, G. Mestroni, *in:Transition Metals for Organic Synthesis: Building Blocks and Fine Chemicals(Eds M.Beller, C.Bolm)*, Wiley-VCH, Weinheim, Germany, 1999, 97.

13 S. Günnaz, N. Özdemir, S. Dayan, O. Dayan, B. Cetinkaya, *Organometallics*, 2011, **30**, 4165.

14 P. Wang, C. H. Leung, D. . Ma, S. C. Yan, C. M. Che, *Chem. Eur. J,* 2010, **16**, 6900.

15 a) Y. X. Chi, S. Y. Niu, J. Jin, R. Wang, Y. Li, *Dalton Trans*, 2009, **37**, 7653; b) Y. X. Chi, S. Y. Niu, Z. L. Wang, J. Jin, *Eur. J. Inorg. Chem*, 2008, **5**, 2336-2343; c) L. P. Sun, S. Y. Niu, J. Jin, G. D. Yang, L. Ye, *Eur. J. Inorg. Chem*, 2007, **24**, 3845; d) L. P. Sun, S. Y. Niu, J. Jin, G. D. Yang, L. Ye, *Eur. J. Inorg. Chem*, 2006, **22**, 5130.

16 a) Y. Zhou, W. Chen, D. Wang, *J. C. S.Dalton Trans*, 2008, **11**, 1444; b) D. Plaul, E. T. Spielberg, W. Z. Plass, *Anorg. Allg. Chem*, 2010, **636**, 1268; c) L. T. Ghoochany, S. Farsadpour, Y. Sun, W. R. Thiel, *Eur. J. Inorg. Chem*, 2011, **23**, 3431; d) P. Wang, C. H. Leung, D.L. Ma, S. C. Yan, C. M. Che, *Chem. Eur. J*, 2010, **16**, 6900; e) Y. Luo, Z. Chen, R. Tang, L. Xiao, *Chem. Reac. Eng. Tech*, 2006, **22**, 549; f) Y. Luo, L. Xiao, Z. Chen, W. Huang, X. Tang, *Chem. Res. App*, 2008, **20**, 299.

17 L. P. Sun, S. Y. Niu, J. Jin, G. D. Yang, L. Ye, *Eur. J. Inorg. Chem,* 2006, **22**, 5130.

18 G. M. Sheldrick, *SADABS, Program for Empirical Absorption Correction for Area Detector Data*, University of Göttingen: Göttingen, Germany, 1996.

19 G. M. Sheldrick, *SHELXS 97, Program for Crystal Structure Refinement*, University of Göttingen: Göttingen, Germany, 1997.

20 J. Marrot, K. Barthelet, C. Simonnet, D. Riou, *C. R. Chimie*, 2005, **8**, 971.

21 A. W. Addison, T. N. Rao, *J. Chem. Soc. Dalton Trans,* 1984, **7**, 1349.

22 Z. P. Li, Y. H. Xing, Y. Z. Cao, X. Q. Zeng, M. F. Ge, S. Y. Niu, *Polyhedron,* 2009, **28**, 865.

23 a) S. L. Li, Y. Q. Lan, J. F. Ma, Y. M. Fu, J. Yang, G. J. Ping, J. Liu, Z. M. Su, *Cryst. Growth Des*, 2008, **8**, 1610; b) Z. Su, J. Xu, J. Fan, D. J. Liu, Q. Chu, M. S. Chen, S. S. Chen, G. X. Liu, X. F. Wang, W.Y. Sun, *Cryst. Growth Des,* 2009, **9**, 2801; c) X. L. Wang, C. Qin, E. B. Wang, Y. G. Li, N. Hao, C.W. Hu, L. Xu, *Inorg. Chem*, 2004, **43**, 1850; d) X. Y. Cao, J. Zhang, Z. J. Li, J.K. Chen, Y.G. Yao, *CrystEngComm*, 2007, **9**, 806.

24 L. Kronik, Y. Shapira, *Surface Science Reports*, 1999, **37**, 1.

25 a) W. H. Brattain, *Phys. Rev*., 1947, **72**, 345; b) W. H. Brattain, J. Bardeen, *Bell System Tech. J*, 1953, **32**, 1; c) C. G. B. Garrett, W. H. Brattain, *Phys. Rev*, 1955, **99**, 376; d) L. Kronik, Y. Shapira, *Surf. Interface Anal,* 2001, **31**, 954.

26 W. Chen, H. M. Yuan, J. Y. Wang, Z. Y. Liu, J. J. Xu, M. Yang, J. S. Chen, *J. Am. Chem. Soc*, 2003, **125**, 9266.

27 a) J. Zhang, D. J. Wang, T. S. Shi, B. H. Wang, J. Z. Sun, T. J. Li, *Thin Solid Films,* 1996, **284/285**, 596-599; b) H. F. Mao, H. J. Tian, Q. F. Hou, H. J. Xu, *Thin Solid Films*, 1997, **300**, 208.

28 a) B. Liu, Z.-T. Yu, J. Yang, H. Wu, Y.-Y. Liu, J.-F. Ma, *Inorg. Chem*, 2011, **50**, 8967; b) H. Lin, P. A. Maggard, *Inorg. Chem*, 2008, **47**, 8044; c) W.-Q. Kan, B. Liu, J. Yang, Y.-Y. Liu, J.-F. Ma, *Cryst. Growth Des*, 2012, **12**, 2288; d) Q. Wu, W. L. Chen, D. Liu, C. Liang, Y. G. Li, S. W. Lin and E. Wang, *Dalton Trans*, 2011, **40**,

56; e) L.-L. Wen, F. Wang, J. Feng, K.-L. Lv, C.-G. Wang and D.-F. Li, *Cryst. Growth Des*, 2009, **9**, 3581; f) K. L. Lv and Y. M. Xu, *J. Phys. Chem. B*, 2006, **110**, 6204; g) L.-L. Wen, F. Wang, J. Feng, K.-L. Lv, C.-G. Wang and D.-F. Li, *Cryst. Growth Des*, 2009, **9**, 3581; h) M. Q. Hu and Y. M. Xu, *Chemospher.*, 2004, **54**, 431; i) K. L. Lv and Y. M. Xu, *J. Phys. Chem. B*, 2006, **110**, 6204.